# Polymerization of Anionic Wormlike Micelles

Zhiyuan Zhu,[†] Yamaira I. González,[‡,||] Hangxun Xu,[†] Eric W. Kaler,[‡] and Shiyong Liu*[,†,§]

*Department of Polymer Science and Engineering, University of Science and Technology of China, Hefei 230026, Anhui Province, P.R. China, Department of Chemical Engineering, University of Delaware, Newark, Delaware 19716, and The Hefei National Laboratory for Physical Sciences at Microscale, Hefei, Anhui, P.R. China*

*Received September 1, 2005. In Final Form: November 16, 2005*

Polymerizable anionic wormlike micelles are obtained upon mixing the hydrotropic salt *p*-toluidine hydrochloride (PTHC) with the reactive anionic surfactant sodium 4-(8-methacryloyloxyoctyl)oxybenzene sulfonate (MOBS). Polymerization captures the cross-sectional radius of the micelles (∼2 nm), induces micellar growth, and leads to the formation of a stable single-phase dispersion of wormlike micellar polymers. The unpolymerized and polymerized micelles were characterized using static and dynamic laser light scattering, small-angle neutron scattering, $^1$H NMR, and stopped-flow light scattering. Stopped-flow light scattering was also used to measure the average lifetime of the unpolymerized wormlike micelles. A comparison of the average lifetime of unpolymerized wormlike micelles with the surfactant monomer propagation rate was used to elucidate the mechanism of polymerization. There is a significant correlation between the ratio of the average lifetime to the monomer propagation rate and the average aggregation number of the polymerized wormlike micelles.

## Introduction

Hydrotropic molecules can be used as additives in surfactant solutions to promote structural transitions such as the transition from micelles to vesicles or from spherical micelles to wormlike micelles.[1−5] Hydrotropes bind strongly to the surfactant headgroup region of the micelles, which reduces the headgroup−headgroup repulsions and causes spherical micelles to be transformed into aggregates of lower curvature.[6,7] Although the effect of hydrotropes on the formation of wormlike micelles in mixtures of cationic surfactant solutions has been extensively studied,[1−5] much less is known regarding the ability of anionic surfactants to form wormlike micelles upon the addition of a hydrotropic salt. The majority of these studies have focused on sodium dodecyl sulfate (SDS) solutions,[8,9] although more recently anionic wormlike micelles made of sodium oleate in the presence of triethylammonium chloride have been reported.[10]

Wormlike micelles display rheological behavior similar to that of flexible polymers, and this is often a desired property for a number of applications.[11−16] However, the use of wormlike micelles in applications is often limited by the fact that the equilibrium between the micelles and unimers is governed by a delicate balance of intermolecular forces, which can be easily disrupted by changes in temperature, dilution, salt concentration, and the addition of oils or polymers.[6,7] This issue of stability can be addressed by chemically fixing the structure of the wormlike micelles through the polymerization of a polymerizable group located either in the hydrophobic portion of the micelles, in the micelle headgroups, or in the micelle counterions.[17−21]

Reports on the polymerization either *in* or *of* wormlike micelles are rare.[17−22] Kline et al. showed that rodlike micelles made of cetyltrimethylammonium 4-vinylbenzoate (CTVB) could be polymerized.[18−21] The counterion used contains a polymerizable vinyl group that binds to the hydrophilic ammonium headgroup of the wormlike micelles. Upon polymerization, the linked counterions form a shell that retains the cross-sectional structure of the resulting micelle, although there is a reduction in the overall length of the polymerized micelles. Becerra et al.[22] reported the polymerization of styrene in wormlike micelles of cetyltrimethylammonium tosylate (CTAT). They concluded that the polymerization of a hydrophobic monomer in the core of the micelles cannot capture the original micellar microstructure, especially at high CTAT concentrations.[22]

Previously,[17] we reported the structural fixation of stable wormlike micelles formed in mixtures of a polymerizable cationic surfactant with an oppositely charged hydrotropic salt. The tail of these wormlike micelles can be successfully polymerized to yield stable dispersions of polymerized micelles whose structure and properties are insensitive to dilution. The cross-sectional radius of the wormlike assemblies (∼2 nm) remains constant,

* To whom correspondence should be addressed. E-mail: sliu@ustc.edu.cn.

† University of Science and Technology of China.

‡ University of Delaware.

§ The Hefei National Laboratory for Physical Sciences at Microscale.

|| Current address: DuPont Central Research and Development, Experimental Station, Wilmington, Delaware 19880.

(1) Rehage, H.; Hoffmann, H. *J. Phys. Chem.* **1988**, *92*, 4712.
(2) Ait Ali, A.; Makhloufi, R. *Phys. Rev. E* **1997**, *56*, 4474.
(3) Soltero, J. F. A.; Puig, J. E. *Langmuir* **1996**, *12*, 2654.
(4) Liu, S.; González, Y. I.; Danino, D.; Kaler, E. W. *Macromolecules* **2005**, *38*, 2482.
(5) Carver, M.; Smith, T. L.; Gee, J. C.; Delichere, A.; Caponetti, E.; Magid, L. J. *Langmuir* **1996**, *12*, 691.
(6) Evans, D. F.; Wennerstrom, H. *The Colloidal Domain: Where Physics, Chemistry, Biology, and Technology Meet*; VCH Publishers: New York, 1994.
(7) Lindman, B.; Wennerström, H. *Top. Curr. Chem.* **1980**, *87*, 1.
(8) Ni, C.; Hassan, P. A.; Kaler, E. W. *Langmuir* **2005**, *21*, 3334.
(9) Hassan, P. A.; Raghavan, S. R.; Kaler, E. W. *Langmuir* **2002**, *18*, 2543.
(10) Kalur, G. C.; Raghavan, S. R. *J. Phys. Chem. B* **2005**, *109*, 8599.
(11) Manohar, C.; Rao, U. R. K.; Valaulikar, B. S.; Iyer, R. M. *J. Chem. Soc., Chem. Commun.* **1986**, *5*, 379.
(12) Candau, S. J.; Hirsch, E.; Zana, R.; Adam, M. *J. Colloid Interface Sci.* **1988**, *122*, 430.
(13) Lin, Z. *Langmuir* **1996**, *12*, 1729.
(14) Cates, M. E. *Macromolecules* **1987**, *20*, 2289.
(15) Hoffmann, H.; Ulbricht, W. *J. Colloid Interface Sci.* **1989**, *129*, 388.
(16) Brackman, J. C.; Engberts, J. B. F. N. *J. Am. Chem. Soc.* **1990**, *112*, 2.
(17) Liu, S.; González, Y. I.; Danino, D.; Kaler, E. W. *Macromolecules* **2005**, *38*, 2482.
(18) Kline, S. R. *Langmuir* **1999**, *15*, 2726.
(19) Gerber, M. J.; Kline. S. R.; Walker, L. M. *Langmuir* **2004**, *20*, 8510.
(20) Biggs, S.; Kline, S. R.; Walker, L. M. *Langmuir* **2004**, *20*, 1085.
(21) Kline, S. R. *J. Appl. Crystallogr.* **2000**, *33*, 618.
(22) Becerra, F.; Soltero, J. F. A.; Puig, J. E.; Schulz, P. C.; Esquena, J.; Solans, C. *Colloid Polym. Sci.* **2003**, *282*, 103−109.

10.1021/la052384i CCC: $33.50 
Published on Web 12/21/2005

but their length increases considerably upon polymerization. Using a similar approach, we report here the growth and structural fixation of anionic wormlike micelles made of a polymerizable anionic surfactant, namely, sodium 4-(8-methacryloyloxyoctyl)-oxybenzene sulfonate (MOBS), and the hydrotropic salt *p*-toluidine hydrochloride (PTHC). Polymerization leads to the uniaxial growth of the micelles and allows for the formation of stable dispersions of polymerized wormlike micelles. The average lifetime of the unpolymerized wormlike micelles was also measured using the stopped-flow method to further understand the interplay of the dynamic exchange of micelle−surfactant unimers and the fast surfactant monomer propagation rate on the change in micellar length during polymerization.

## Materials and Methods

**Materials.** 1,8-Octanediol, phenol-4-sulfonic acid sodium dehydrate, and *p*-toluidine hydrochloride (PTHC) were purchased from Fluka. The initiator, 2,2′-azobis(2-methylpropionamide) dihydrochloride (V50, Wako Pure Chemical Industries, Ltd), was recrystallized from methanol. Dowex 50W-X8(H) ion-exchange resin was obtained from BDH. Methacryloyl chloride was prepared by reacting methacrylic acid with phosphorus trichloride.[23]

**Preparation of the Polymerizable Surfactant.** *8-Bromo-1-octanol.* A mixture of 1,8-octanediol (25.38 g, 0.174 mol) and 40% aqueous hydrobromic acid (75 mL) was held at 75 °C for 72 h while being continuously extracted with cyclohexane. The cyclohexane extract (500 mL) was washed with a 5% aqueous sodium bicarbonate solution (250 mL), water (250 mL), and brine (250 mL) and then dried with $MgSO_4$. The solvent was removed in vacuo to obtain pure 8-bromo-1-octanol in 85% yield.

*4-(8-Hydroxyoctanyl)oxybenzene Sulfonic Acid (HOBS).* Phenol-4-sulfonic acid sodium dehydrate, KOH (7.07 g, 0.126 mol), and $H_2O$ (120 mL) were mixed in a 500 mL round-bottomed flask equipped with a condenser. 8-Bromo-1-octanol (30.15 g, 0.12 mol) in 180 mL of ethanol was added, and the reaction mixture was refluxed overnight. A white precipitate of 4-(8-hydroxyoctyl)oxybenzene sulfonate formed when the reaction mixture was cooled in an ice water bath. The solid was filtered and washed with chloroform to remove 8-bromo-1-octanol and was purified by recrystallization from hot water. The resulting white product was dissolved in hot distilled water and eluted through a Dowex 50WX8(H) ion-exchange column preheated to 60−70 °C. After elution, 4-(8-hydroxyoctyl)-oxybenzene sulfonate was converted to its sulfonic acid form. The effluent was freeze dried to obtain a white, fluffy solid.[24]

*Sodium 4-(8-methacryloyloxyoctyl)oxybenzene Sulfonate (MOBS).* 4-(8-hydroxyoctyl)oxybenzene sulfonic acid (20 g, 0.066 mol) was dissolved in dry THF (200 mL) in a 500 mL, three-necked, round-bottomed flask equipped with an air-leak and dropping funnel. Methacryloyl chloride (15.14 mL, 0.156 mol) and a solution of hydroquinone (0.14 g, 0.00127mol) in dry THF (30 mL) were added dropwise. The reaction mixture was stirred for 48 h under $N_2$ protection. Unreacted methacryloyl chloride and THF were removed in vacuo. Ether was added to the orange-brown oil residue, and then a saturated brine solution was added to convert the sulfonic acid into its sodium salt form. MOBS was washed with ether and dried before it was recrystallized from methanol. Purified MOBS was obtained as a white powder with an overall yield of 70%. The chemical structures of the synthesized MOBS and PTHC are shown in Figure 1. Their structures and purity were verified by $^1$H NMR. The spectra of these species are discussed in detail in the $^1$H NMR discussion below.

**Polymerization of Wormlike Micelles.** Micelles for polymerization were prepared with water or $D_2O$ and depleted of oxygen by bubbling with nitrogen for about 20 min. After dissolution at room temperature of the desired MOBS and PTHC compositions, the solution mixtures were heated to 60 °C. The water-soluble initiator

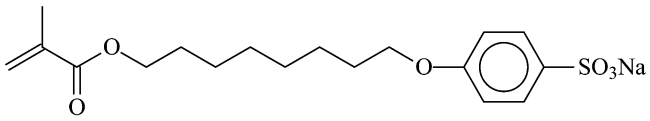


MOBS

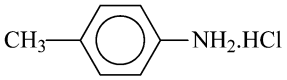


PTHC

**Figure 1.** Chemical structures of sodium 4-(8-methacryloyloxy-octyl)oxybenzene sulfonate (MOBS) and *p*-toluidine hydrochloride (PTHC).

V50, predissolved in degassed water or $D_2O$, was injected (the molar ratio of MOBS to V50 was fixed at 100), and the polymerization was carried out at 60 °C for 1 h.

**Laser Light Scattering (LLS).** A commercial LLS spectrometer (ALV/SP-125) equipped with an ALV-5000 multitau digital time correlator and a He−Ne laser (Uniphase, 22 mW at $\lambda = 632.8$ nm) was used. Samples were measured at 25 °C. Dynamic LLS measurements were made at eight different angles ranging from 15 to 150°. Each intensity−time correlation function was analyzed by the method of cumulants to provide the average decay rate $\langle\Gamma\rangle = q^2D_a$ and the normalized variance $\nu = [(\langle\Gamma^2\rangle - \langle\Gamma\rangle^2)/\langle\Gamma\rangle^2]$, which is a measure of the width of the distribution of the decay rates.[38] Here, $D_a$ is the apparent diffusion coefficient, and $q$ is the magnitude of the scattering vector given by $q = (4\pi n/\lambda)\sin(\theta/2)$, where $n$ is the refractive index of the solvent, $\lambda$ is the wavelength of light, and $\theta$ is the scattering angle. Each stock solution of pure surfactant and salt was filtered through 0.45 $\mu$m Millipore Acrodisc-12 filters prior to preparing samples.

In static LLS, the angular dependence of the excess absolute time-averaged scattered light intensity, known as the Rayleigh ratio $R_{vv}(q)$, of a series of diluted polymerized vesicle solutions (concentrations ranging from $9.8 \times 10^{-5}$ to $2.2 \times 10^{-4}$ g/mL) led to the apparent weight-average molar mass $M_{w,app}$ and the root-mean square $z$-average radius of gyration $\langle R_g^2\rangle_z^{1/2}$ (written as $R_g$). The d$n$/d$c$ value (0.169 mL·g$^{-1}$) of polymerized wormlike micelles was measured at 25 °C using an interferometric refractometer ($\lambda = 632.8$ nm) for a range of concentrations.

**Small-Angle Neutron Scattering (SANS).** SANS measurements were made at the National Institute of Standards and Technology (NIST) in Gaithersburg, MD. An average radiation wavelength of 6 Å with a spread of 11% was used. Samples were held at 25 °C in quartz "banjo" cells with 1 mm path lengths. Three sample−detector distances were used to give a scattering vector range of 0.005−0.5 Å$^{-1}$. The data were corrected for detector efficiency, background, and empty cell scattering and placed on an absolute scale using NIST procedures.[25] The semiflexible model uses Pedersen and Schurtenberger's calculation of the form factor for a wormlike

(23) Labinger, J. A. In *Comprehensive Organic Synthesis*; Trost, B. M., Fleming, I., Eds.; Pergamon Press: Oxford, England, 1991.
(24) Xu, X. J.; Goh, H. L.; Siow, K. S.; Gan, L. M. *Langmuir* **2001**, *17*, 6077.
(25) Barker, J. G.; Pedersen, J. S. *J. Appl. Crystallogr.* **1995**, *28*, 105.
(26) Pedersen, J. S.; Schurtenberger, P. *Macromolecules* **1996**, *29*, 7602.
(27) Liu, S.; Gonzalez, Y. I.; Kaler, E. W. *Langmuir* **2003**, *19*, 10732.
(28) Bhat, M.; Gaikar, V. G. *Langmuir* **1999**, *15*, 4740.
(29) Chu, B. *Laser Light Scattering: Basic Principles and Practice*, 2nd ed.; Academic Press: Boston, 1991.
(30) Brown, W., Ed. *Light Scattering: Principles and Development*;; Clarendon Press: Oxford, England, 1996; Chapter 1.
(31) Teraoka, I. *Polymer Solutions: An Introduction to Physical Properties*, John Wiley & Sons: New York, 2002; Chapter 1.
(32) James, A. D.; Robinson, D. H.; White, N. C. *J. Colloid Interface Sci.* **1977**, *59*, 328.
(33) Tondre, C.; Lang, J.; Zana, R. *J. Colloid Interface Sci.* **1975**, *52*, 372.
(34) Hoffmann, H.; Nagel, R.; Platz, G.; Ulbricht, W. *Colloid Polym. Sci.* **1976**, *254*, 812.
(35) Adair, D. A. W.; Reinsboragh, V. C.; Plavac, N.; Valleau, J. P. *Can. J. Chem.* **1974**, *52*, 429.
(36) Jonsson, B.; Lindman, B.; Holmberg, K.; Kronberg, B. *Surfactants and Polymers in Aqueous Solutions*; Wiley: New York, 1998.
(37) Lessner, E.; Frahm, J. *J. Phys. Chem.* **1982**, *86*, 3032.
(38) Lessner, E.; Teubner, M.; Kahlwelt, M. *J. Phys. Chem.* **1981**, *85*, 1529.

chain with excluded-volume interactions. This model allows the estimation of the contour length ($L_c$) and the persistence length ($l_p$) of the micelle, which are an indication of micellar flexibility.[26] The SANS modeling details are described in a previous publication.[17]

**$^1$H NMR Spectroscopy.** $^1$H NMR measurements were performed at 25 °C on a Bruker AC300 NMR spectrometer (resonance frequency of 300 MHz for $^1$H) operating in the Fourier transform mode.

**Stopped-Flow Light Scattering.** Stopped-flow studies were carried out using a Bio-Logic SFM300/S stopped-flow instrument. The SFM-300/S is a three-syringe (10 mL) instrument in which all step-motor-driven syringes (S1, S2, S3) can be operated independently to carry out single to double mixing. This device is attached to the MOS-250 spectrometer, and the collected kinetic data are fitted using the program Biokine (Bio-Logic). For light-scattering detection, both the excitation and emission wavelengths were adjusted to 335 nm with 10 nm slits. Either an FC-08 or an FC-15 flow cell was used, and the typical dead times were about 1.1 and 2.6 ms, respectively.

**Surface Tensiometry.** Equilibrium surface tensions were measured using a JK99B tensiometer with a platinum plate. The measuring accuracy of the device as reported by the manufacturer is ±0.1 mN/m. The surface tension of pure water (ca. 71 mN/m) was checked periodically between measurements. The reported surface tension at each concentration was the average of three to five measurements that were taken after allowing each of the solutions to equilibrate in the instrument at a temperature of 25.0 ± 0.1 °C.

## Results and Discussion

Pure MOBS surfactant in water has a critical micelle concentration (cmc) of 13.4 mM at 25 °C. With the addition of PTHC, the critical aggregation concentration (cac) of MOBS as measured by surface tension monotonically drops from 13.4 mM (at $x_{PTHC} = 0$) to 5.7 mM (at $x_{PTHC} = 1.0$), where $x_{PTHC}$ is defined as the molar ratio of PTHC to MOBS. (See Figure S1 in Supporting Information.) This reduction in cac is relevant because the stability of polymerized wormlike solutions must be probed for concentrations much lower than the cac.

Below the cmc and cac, isotropic micellar solutions of low viscosity form, but for MOBS concentrations ranging from 10 to 20 to 100 mM and for [PTHC]/MOBS] molar ratios (i.e., $x_{PTHC} \geq 0.7$), the samples display a slightly bluish tinge that indicates apparent micellar growth (i.e., a transition from spherical to wormlike micelles). At $x_{PTHC} > 1.2$, a turbid dispersion is formed that eventually phase separates. This phase behavior is similar to that reported by Hassan et al. for mixtures of SDS and PTHC.[9] In that case, a bluish tinge is visually discernible at [PTHC]/[SDS] molar ratios as low as 0.4, and upon addition of PTHC to SDS, a 1:1 complex forms followed by the presence of a precipitate region for [PTHC]/[SDS] molar ratios higher than 1.[9] Clearly, increasing the electrostatic interactions between the hydrotropic salt and surfactant headgroup drives the transition from spherical micelles to wormlike micelles to precipitate.

## $^1$H NMR Studies

$^1$H NMR studies show that the formation of SDS wormlike micelles induced by PTHC results from the insertion of this hydrotrope into the micelles.[9] Here, we expect PTHC to insert into the micelles in a similar way. Furthermore, because the polar headgroups of MOBS and PTHC both bear one benzene ring, $\pi-\pi$ interactions between the benzene ring of MOBS and the benzene ring of PTHC are likely. Such interactions should be reflected in significant changes in the corresponding NMR signals as compared to the signals of each of the pure species in solution.

Thus, $^1$H NMR spectra of MOBS, PTHC, and mixtures of these species in $D_2O$ were measured (Figure 2). In the spectrum

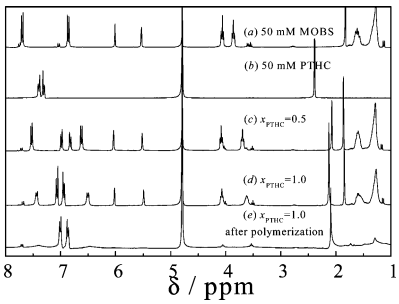


**Figure 2.** $^1$H NMR spectra of a 50 mM MOBS solution, a 50 mM PTHC solution, MOBS/PTHC mixtures, and a polymerized wormlike micellar solution. The MOBS concentration in the mixture is constant at 50 mM.

of 50 mM PTHC, the resonances at $\delta = 7.38-7.40$ ppm are ascribed to the two ortho protons on the benzene ring, whereas the signals at $\delta = 7.29-7.31$ ppm are ascribed to the aromatic meta protons. The three methyl protons at the para position are observed at $\delta = 2.39$ ppm (Figure 2b). In the mixture of 25 mM PTHC with 50 mM MOBS ($x_{PTHC} = 0.5$), the ortho and meta protons as well as the *p*-$CH_3$ resonances of PTHC are both shifted upfield from their original positions to 6.99−6.97, 6.84−6.82, and 2.08 ppm, respectively (Figure 2c). This ∼0.4 ppm upfield shift is very large compared to that seen for mixtures of SDS/PTHC. For the latter, the upfield shift is about 0.1 ppm.[9,28] At $x_{PTHC} = 0.5$, the signals for the protons on the MOBS benzene ring at 7.8−7.6 and 6.9−6.7 ppm also shift upfield about 0.2−0.3 ppm. These shifts are evidence of a strong interaction between the polar heads of MOBS and PTHC, which is partially due to the $\pi-\pi$ interaction between the benzene ring of MOBS and the benzene ring of PTHC. Such interactions would enhance the insertion and binding of PTHC to the micelle surface.

At $x_{PTHC} = 1.0$ (Figure 2d), the signals of benzene ring protons of MOBS move further upfield, whereas the ortho and meta protons as well as the *p*-$CH_3$ resonances of PTHC all shift downfield slightly compared to that at $x_{PTHC} = 0.5$ (Figure 2c). The less-prominent upfield shift is probably due to the contribution of free (unbound) counterions to the total signal.[17]

With increasing PTHC, the triplet observed at around $\delta = 3.86$, which is the resonance of two protons in the $-CH_2O-PhSO_3Na$ group of MOBS, also shows an increasing upfield shift. This shift agrees with the upfield shift of the *p*-$CH_3$ resonance of PTHC and clearly indicates that PTHC strongly binds to the surface of the micelles with its benzene ring and *p*-$CH_3$ group intercalated into the micellar interior (in close proximity with benzene ring of MOBS), whereas the $-NH_3^+$ headgroup of PTHC is protruding from the micelle surface.

Significant changes are also seen in the NMR spectra of the micelles before and after polymerization, and these are evidence of the changes suffered by the micelles during the reaction. Before polymerization (Figure 2a), the signals at $\delta = 1.83$ ($CH_3$ on the methacrylate group of MOBS) and $\delta = 5.4-6.0$ ($CH_2$ on the double bond) characteristic of protons of methacrylate groups can be clearly seen. After polymerization (Figure 2e), all of the signals characteristic of the methacrylate groups disappear, which indicates complete polymerization of the surfactant monomers. Another interesting feature of the polymerized wormlike micelles is that the signals due to the surfactant tail (<1.8 ppm) are barely noticeable, suggesting that the mobility of the surfactant tail has been greatly restricted by polymerization. This is understandable given that polymerization has covalently linked the hydrophobic tails together such that the fluidity of the hydrophobic core is largely reduced.[17,27]

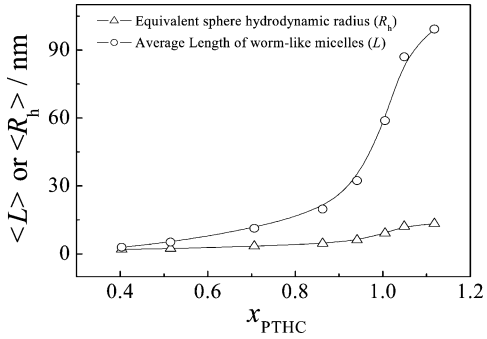


**Figure 3.** Calculated average length of the wormlike micelles ($L$) and the average equivalent average sphere hydrodynamic diameter ($\langle R_h \rangle$) as a function of the molar ratio of PTHC to surfactant, $x_{PTHC}$.

After polymerization, the resonances from protons on the benzene ring of MOBS appear only as a broad band when compared to that observed for the unpolymerized wormlike micelles. A more careful examination of parts d and e of Figure 2 shows that the ortho and meta protons as well as the *p*-$CH_3$ resonances of PTHC show further upfield shifts, indicating their stronger intercalation with MOBS after polymerization. This also partially explains the broadening of the MOBS benzene proton signals after structural fixation. As discussed in the following section, much longer wormlike micelles are obtained after polymerization, and this size increase may also lead to the broadening of $^1$H NMR signals.

## LLS Studies

Dynamic LLS was used to probe the variation in micellar size upon addition of PTHC to MOBS. The approach has been previously described by Hassan et al.[9] and Liu et al.[17] and has proven to be applicable to the characterization of relatively short unpolymerized micelles. Briefly, from the average decay rate $\bar{\Gamma}$ and $q$, the apparent diffusion coefficient, $D_a$, of the micelles can be determined (Figure S2 in Supporting Information). $D_a$ decreases with increasing $x_{PTHC}$, which suggests the formation of wormlike micelles of increasing length.[9,17]

To extract information about the micellar size (i.e., the length of the wormlike micelles) from $D_a$, the effect of interactions between neighboring micelles was considered, and a set of equations outlined by Hassan et al.[9] that relate the micellar length ($L$) to $D_a$ was solved. The micelle length was calculated via an iterative procedure under the assumption that the cross-sectional radius is preserved. The micellar radius ($r$) was set at 2.05 nm, which is roughly the length of the hydrocarbon chain of MOBS.[6]

Figure 3 shows that the addition of PTHC leads to significant micellar growth. When $x_{PTHC} < 0.7$, the growth is moderate; upon further increasing $x_{PTHC}$, there is a monotonic increase in the micellar length up to ~100 nm at $x_{PTHC} = 1.1$, which corresponds to an axial ratio of $p = L/2r \approx 25$. The dynamic LLS data thus suggest a structural transition from spherical to wormlike micelles.

The variation of the scattering intensities of the polymerized wormlike micelles upon dilution reveals an inflection point at ~2.5 mM, which likely signals the onset of micellar overlapping (Figure 4).[6,27] At lower concentrations (<2.5 mM), the scattering intensity varies linearly with concentration, whereas at higher concentrations the slope decreases considerably. Consequently, all of the light-scattering measurements of the polymerized wormlike micelles were made at concentrations below 2.5 mM. Polymerized wormlike micelles exhibit a much lower $D_a$ (Figure S2 in Supporting Information) than the unpolymerized ones, which indicates the presence of substantially longer wormlike micelles in solution after polymerization.

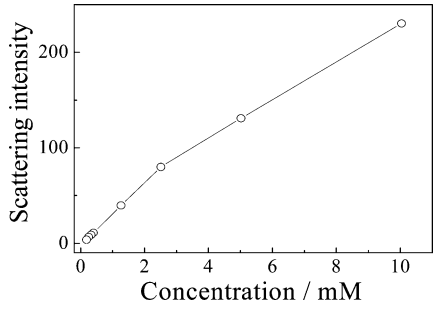


**Figure 4.** Scattering intensity vs concentration for wormlike micelles polymerized at 50 mM MOBS and $x_{PTHC} = 1.0$ during dilution.

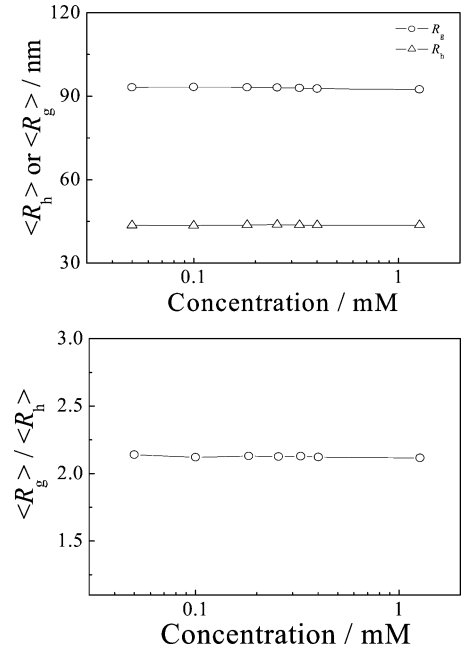


**Figure 5.** Variation of the values of the apparent $\langle R_g \rangle$, $\langle R_h \rangle$, and $\langle R_g \rangle / \langle R_h \rangle$ with concentration during dilution. The polymerization was carried out at 50 mM MOBS with $x_{PTHC} = 1.0$.

Figure 5 shows the concentration dependence of the average hydrodynamic radius ($\langle R_h \rangle$, directly measured by dynamic LLS) of the polymerized wormlike micellar solutions at $x_{PTHC} = 1.0$. It is clear that $\langle R_h \rangle$ remains nearly constant in the concentration range from 0.05 to 1.25 mM, indicating that the wormlike micellar structure remains after polymerization. If the structural fixation had not been successful, then the wormlike micelles would have dissociated into unimers at concentrations well below the cac of MOBS at $x_{PTHC} = 1.0$ (5.7 mM). After the structure of the wormlike micelles is fixed, static LLS (Figure 6) can be used to calculate their weight-average molar mass ($M_w$) and average radius of gyration ($\langle R_g \rangle$). The data indicate that $M_w \approx 3.1 \times 10^6$ g·mol$^{-1}$ and $\langle R_g \rangle \approx 92$ nm, results that suggest that each polymerized wormlike micelle contains approximately 7900 MOBS surfactant molecules. As also shown in Figure 5, the apparent $\langle R_g \rangle$ of the polymerized wormlike micelles remains constant (~92 nm), whereas the average sphere hydrodynamic radius $\langle R_h \rangle$ is ~44 nm. The ratio of $\langle R_g \rangle / \langle R_h \rangle$ reflects the density distribution of the scatterers in space; $\langle R_g \rangle / \langle R_h \rangle \approx 1.5$ for monodisperse random coil chains and ~1.3−4.0 for elongated micelles.[29−31] Here the high value of $\langle R_g \rangle / \langle R_h \rangle \approx 2.1$ is consistent with an extended wormlike micellar structure.[6]

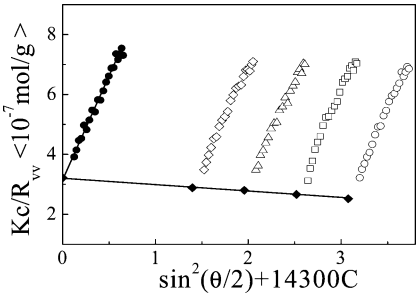


**Figure 6.** Zimm plots of polymerized wormlike micelles (polymerized at 50 mM MOBS with a molar ratio of $x_{PTHC} = 1.0$). A series of dilute polymerized wormlike micelle dispersions (concentrations ranging from $9.8 \times 10^{-5}$ to $2.2 \times 10^{-4}$ g/mL) were used for the SLS measurements.

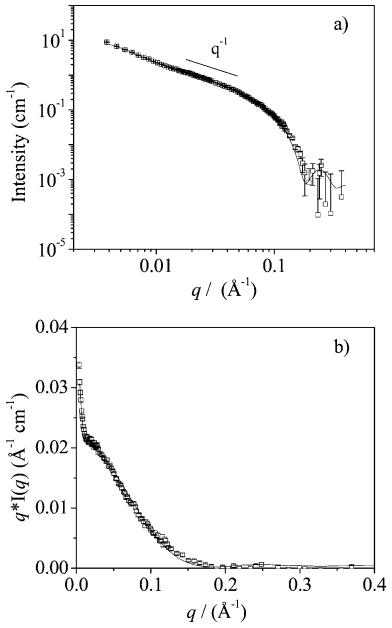


**Figure 7.** (a) SANS spectra of the polymerized wormlike micelles. The solid line represents the best fit to the experimental data using a semiflexible model with excluded volume interactions. (b) Holtzer plot of polymerized wormlike micelles, with the upturn at low $q$ values indicating a semiflexible wormlike microstructure. The polymerization was carried out at 50 mM MOBS with a molar ratio of $x_{PTHC} = 1.0$ and then diluted 5-fold.

The polymerized wormlike micelles at low concentrations are well separated from each other. As the concentration $C$ increases, they are concentrated and eventually come into contact. At the so-called overlap concentration ($C^*$), the whole volume of the solution is filled with these wormlike chains. The overlap concentration can be calculated using eq 1, assuming each wormlike chain occupies the volume equal to a sphere with a radius of $\langle R_g \rangle$, so

$$\frac{4}{3}\pi C^* \langle R_g \rangle^3 = \frac{M}{N_A} \tag{1}$$

where $M/N_A$ is the mass of each chain and $N_A$ is Avogadro's number.[31] The calculated value of $C^*$ is 4.0 mM, which is close to the inflection point (2.5 mM) in the plot of the scattered light intensity versus concentration (Figure 4).[17]

**Small-Angle Neutron Scattering (SANS) Studies.** Figure 7a shows the SANS spectrum of the polymerized wormlike micelles, where [MOBS] = 50 mM and $x_{PTHC} = 1.0$. The scattered intensity has a $q^{-1}$ dependence in the intermediate range of $q$, which is the signature of the scattering from 1D objects. The spectrum qualitatively confirms the wormlike micellar structure. Because of the screening effect of PTHC, the SANS intensity profile shows no Coulomb interaction peak at lower $q$ values.

The cross-sectional radius $r_{cs}$ of the wormlike micelles can be obtained by analyzing the intermediate portion of the scattering curve using the Guinier approximation for the form factor (Figure S3 in Supporting Information). The fitting of the linear portions of the cross-sectional Guinier plot of $\ln(Iq)$ versus $q^2$ leads to $r_{cs} \approx 2.2$ nm, which considering experimental uncertainties agrees with the 2.1 nm calculated length of a fully extended MOBS molecule. The best fit using a semiflexible cylinder model to the scattering spectrum yields a cross-sectional diameter $r_{cs}$ of $2.1 \pm 0.1$ nm, a contour length $L_c$ of $203 \pm 15$ nm, a persistence length ($l_p$) of $26 \pm 3$ nm, and a reduced error of 2.0. There is a slight discrepancy in the fit at high $q$ where the scattered intensity is very low. Evidence of the flexibility of the micelles is obtained from a Holtzer plot (Figure 7b), which is constructed to highlight the deviation of the scattering data from that of ideal, rigid cylinders. In this plot, the upturn in the low-$q$ region indicates that the micelles are best described by a semiflexible cylinder model. A rigid cylinder model did not give a good fit to the SANS scattering profile, particularly in the low-$q$ range (data not shown).

For a wormlike chain with a contour length $L_c$ of 203 nm and a persistence length $l_p$ of 26 nm, $L_c \gg l_p$, so the radius of gyration, $R_g$, can be calculated as[31]

$$R_g = \sqrt{L_c l_p} \tag{2}$$

The calculated $R_g$ is ~73 nm, whereas the $\langle R_g \rangle$ determined by static LLS is ~92 nm. The discrepancy between these two values reflects the fact that the surfactant concentration used in SANS was 10 mM, which is higher than the micellar overlap concentration, so the intermicellar interactions should have a large effect on the model calculation, especially in the low-$q$ range. Furthermore, in SANS and static LLS, the number- and weight-averaged values are measured, respectively, and for a polydisperse sample, the weight-average value will be higher.

For the polymerized wormlike micelles, on the basis of the average aggregation number deduced from static LLS, the micellar length deduced from SANS fitting, and the cross-sectional diameter, we estimated the surface area ($a_o$) of the headgroup per MOBS surfactant to be 0.34 nm$^2$. However, using the chemical structure of the MOBS surfactant, the calculated length $l$ and volume $v$ of its hydrocarbon tail are 2.1 and 0.41 nm$^3$, respectively.[6] The estimated packing parameter ($N_s = v/a_o l$) of MOBS in the presence of PTHC (at $x_{PTHC} = 1.0$) is ~0.57, which is close to the theoretical value (0.5) for an infinitely long cylinder.[6,36]

**Stopped-Flow Studies.** The above sections provide detailed structural information about unpolymerized and polymerized wormlike micelles. Here, the formation and dissociation kinetics of wormlike micelles before and after polymerization are discussed. The kinetics of forming spherical micelles has been extensively studied by a variety of methods including stopped-flow,[32] temperature-jump,[33] pressure-jump,[34] and ultrasonic absorption.[35] Reports suggest that a micellar solution can be characterized by two relaxation processes, namely, fast and slow relaxation processes.[6,36] The fast relaxation ($\tau_1$, which is on the order of microseconds) is associated with the exchange between monomers in the micelles and in the dispersion medium. The slow relaxation ($\tau_2$, which is on the order of milliseconds) is related to the formation and breakdown of the micelles. In other words, $\tau_1$ and $\tau_2$ are respectively related to the residence time of a surfactant molecule in the micelle and the average lifetime

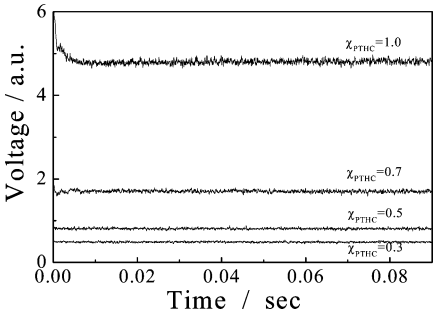


**Figure 8.** Time dependence of the light-scattering intensity after mixing MOBS with PTHC at different molar ratios, $x_{PTHC}$. The final concentration of MOBS is 50 mM.

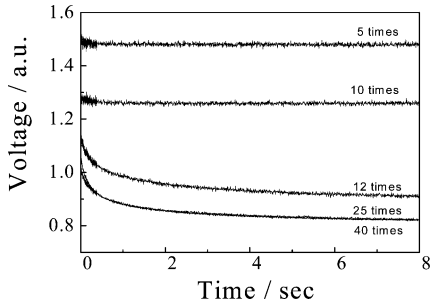


**Figure 9.** Time dependence of the light-scattering intensity of an unpolymerized wormlike micellar solution at different times of dilution with water. The initial wormlike micellar solution contains 50 mM MOBS at $x_{PTHC} = 1.0$.

or stability of the micelle. There are only a few experimental studies of the kinetics of the spherical-to-wormlike micelle transition.[37−40]

*Kinetics of Wormlike Micelle Formation.* The transition from spherical to wormlike micelles upon mixing different amounts of PTHC with MOBS was probed (Figure 8) using a stopped-flow device coupled with light-scattering detection. At low $x_{PTHC}$ ratios, no relaxation was observed at all, whereas at higher $x_{PTHC}$ ratios (>0.7), the relaxation had a negative amplitude that is indicative of a decease in the length or number of wormlike micelles. The expected initial increase in the scattered light intensity due to micelle growth was not observed, which implies that the initial relaxation is too fast to be observed by stopped-flow mixing. Such rapid relaxation must reflect the short hydrocarbon chain of MOBS because we observed a relaxation process with a positive amplitude for SDS solutions upon the addition of PTHC ($\tau$ is typically ∼60 ms at 50 mM SDS and $x_{PTHC} = 0.5$) (data not shown).

*Dissociation Kinetics of Wormlike Micelles before and after Polymerization.* The light-scattering intensity versus time plots of a wormlike solution originally at 50 mM MOBS and $x_{PTHC} = 1.0$ and diluted several times are shown in Figure 9. Up to 10-fold dilution, a relaxation process can barely be detected, which is indicated by the lack of any decay of the intensity with time. With further dilution, (e.g., 12-fold or more), a relaxation process with negative amplitude is observed. Such a transition is most likely due to the dissociation of wormlike micelles to unimers, and the results suggest a cac of MOBS at $x_{PTHC} = 1$ of ∼4−5 mM. Note that this value is in good agreement with the value deduced from the surface tension measurements (∼5.7 mM). Also note that 25- or 40-fold dilution leads to overlapping kinetic traces that are a signature of the complete dissociation

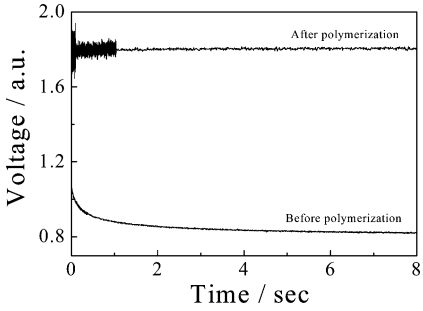


**Figure 10.** Time dependence of the light-scattering intensity after 25-fold dilution with water at 25 °C for polymerized and unpolymerized wormlike micelles. The initial wormlike micellar solution contains 50 mM MOBS at $x_{PTHC} = 1.0$. Higher sampling frequencies are used for the first few seconds.

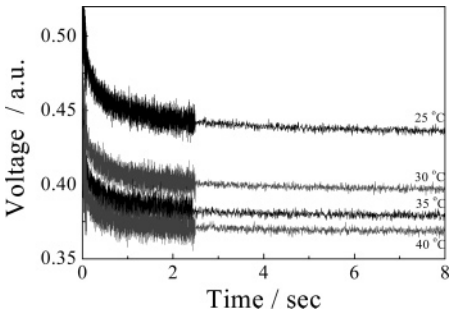


**Figure 11.** Time dependence of the light-scattering intensities after 25-fold dilution with water at different temperatures. The initial wormlike micellar solution contains 50 mM MOBS at $x_{PTHC} = 1.0$. Much higher sampling frequencies are used for the first few seconds.

of the wormlike micelles to unimers. The relatively good agreement between the cac values obtained from surface tensiometry and stopped-flow dilution indicates that both methods reflect the cac of the wormlike micelles. For spherical micelles, this stopped-flow technique for measuring cac values is probably not applicable because micellar dissociation is much more rapid (typically $\tau$ < 1 ms).[6,36]

As expected, the polymerized wormlike micelles exhibit no observable relaxation processes after 25-fold dilution with water (Figure 10). The equilibrium light-scattering intensity is also much higher than that from the unpolymerized micelles, further confirming the successful fixation of the wormlike micellar microstructure. If the micelles were not polymerized, then they would disintegrate into unimers after dilution to concentrations well below the cac.

*Average Micelle Lifetime.* The polymerization of the wormlike micelles was carried out at 60 °C. To deduce the average micelle lifetime or/and stability of the wormlike micelles and to understand the polymerization mechanism, we measured the dissociation kinetics at different temperatures by carrying out 25-fold stopped-flow dilution with water (Figure 11). Analysis yields the estimated dissociation rate constants $k_{diss}$.

The time dependence of the light-scattering intensity $I_t$ can be converted to a normalized function, namely, $(I_\infty - I_t)/I_\infty$ versus $t$, where $I_\infty$ is the value of $I_t$ at an infinitely long time. Empirically, we found that such a function could be well fit by a double-exponential function

$$\frac{I_t - I_\infty}{I_\infty} = a_1 e^{-k_1 t} + a_2 e^{-k_2 t} \qquad (3)$$

where $a_1$ and $a_2$ are the normalized amplitudes ($a_2 = 1 - a_1$) and $k_1$ and $k_2$ are the relaxation constants.[6,35] The mean dissociation

(39) Ilgenfritz, G.; Schneider, Grell, E.; Lewitzki, E.; Ruf, H. *Langmuir* **2004**, *20*, 1620.
(40) Imae, T.; Ikeda, S. *J. Phys. Chem.* **1986**, *90*, 5216.

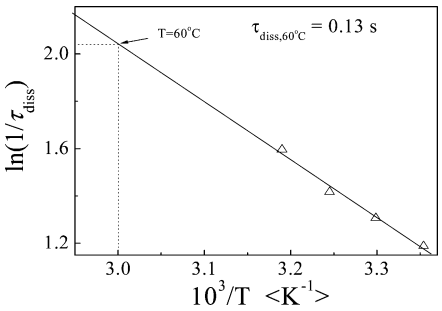


**Figure 12.** Temperature dependence of $\ln(1/\tau_{diss})$ obtained from the data shown in Figure 11.

constant, $k_{diss}$, can be calculated as

$$\frac{1}{k_{diss}} = \frac{a_1}{k_1} + \frac{a_2}{k_2} \tag{4}$$

where $1/k_{diss}$ equals the characteristic delay time $\tau_{diss}$. Figure 12 shows the temperature dependence of $\ln(1/\tau_{diss})$. With increasing temperature, $1/\tau_{diss}$ increases. Extrapolation to the polymerization temperature at 60 °C leads to a good estimate of $\tau_{diss} \approx 0.13$ s. For concentrations near cac, $\tau_{diss}$ should be very close to $\tau_2$.[41,42]

*Polymerization Mechanism.* Wormlike micelles and unimers coexist in dynamic equilibrium. Such a dynamic nature can be better described in terms of the average micelle lifetime (i.e., the time required for the association of surfactant unimers into the micelles). During polymerization, the mean lifetime of the unpolymerized wormlike micelles ($t_m$) can be calculated as[43−45]

$$t_m = N\tau_2 \tag{5}$$

where $N$ is the average aggregation number in each unpolymerized wormlike micelle, which can be estimated from the length (Figure 3) and the cross-sectional radius (2.1 nm) of the wormlike micelles as well as the surface area occupied per surfactant (∼0.36 $nm^2$ per surfactant).[17] Thus, for 50 mM MOBS at $x_{PTHC} = 1.0$, $N$ is ∼2150 and $t_m$ is ∼280 s.

The actual aggregation number of each micelle fluctuates around $N$ as a result of the diffusion of surfactant unimers into and out of the micelle. As discussed in our previous paper,[17] this migration of surfactant is important because the unreacted unimers can move from one micelle to another during polymerization. The time scale for the association of a unimer, $t_a$, is given by $(k^+\text{cac})^{-1}$, where the association rate constant is $k^+ \approx 10^9$ $(\text{M·s})^{-1}$.[45] Thus, $t_a \approx 2 \times 10^{-7}$ s, so unimers are continuously exchanged and thus can be incorporated into the polymerized micelle.

Finally, let us examine the rate of growth of the oligomeric chains. This growth should mainly depend on the propagation time ($t_p$) during which a monomer is added to the growing chain. $t_p \approx (k_p[\text{M}])^{-1}$, where $k_p \approx 1000\ (\text{M s})^{-1}$ for *n*-alkyl methacrylates with a degree of polymerization of 10 or higher and [M] is the monomer concentration.[46] For 50 mM MOBS at $x_{PTHC} = 1.0$, $t_p \approx 2 \times 10^{-2}$ s in the initial stage of the reaction. This value is 4 orders of magnitude smaller than the micelle lifetime (280 s) but much longer than the association time of a surfactant unimer to the micelle ($2 \times 10^{-7}$ s).

The polymerization of wormlike micelles resembles a typical microemulsion polymerization, where monomer-swollen micelles are replaced by wormlike micelles containing polymerizable double bonds inside the hydrophobic core.[47,48] The number of micelles far exceeds the number of radicals. Therefore, the probability of more than one radical entering a micelle is negligible. It is quite likely that radicals formed by the decomposition of water-soluble initiators rapidly partition into the micelles.

Because the propagation time step is 4 orders of magnitude faster than the average micelle lifetime, oligomeric radicals are formed during the average micelle lifetime. The length of these oligomeric radicals, given by the ratio of $t_m/t_p$, is $\sim 10^4$ units. The aggregation number of the polymerized wormlike micelles from 50 mM MOBS at $x_{PTHC} = 1.0$ is 7900. The good agreement between these two values strongly supports the proposed polymerization mechanism for the wormlike micelles, namely, that the average length of polymerized wormlike micelles is mainly determined by $t_m/t_p$ and not by the average length of the original wormlike micelles. One may argue that at lower $x_{PTHC}$ shorter wormlike micelles (lower $N$) are formed with a lower $t_m = N\tau_2$. The situation is more complex because $\tau_2$ also changes with $x_{PTHC}$ for a given MOBS concentration. A detailed investigation of the correlation between $t_m/t_p$ and the aggregation number in the polymerized wormlike micelles is currently ongoing.

## Conclusions

The micellar structural transition from spherical to wormlike anionic micelles can be accomplished upon addition of *p*-toluidine hydrochloride (PTHC), a hydrotropic salt, to aqueous solutions of sodium 4-(8-methacryloyloxyoctyl)oxybenzene sulfonate (MOBS), a polymerizable anionic surfactant. The polymerization of wormlike micelles leads to stable dispersions of polymerized wormlike micelles. After polymerization, the cross-sectional radius remains unchanged (∼2 nm), but the micelle length increases from several tens of nanometers to several hundred nanometers. The average micelle lifetime of the wormlike micelles before polymerization was measured and combined with the surfactant monomer propagation rate to elucidate the mechanism of polymerization.

**Acknowledgment.** This work is supported by an Outstanding Youth Fund (50425310) and a key research grant (20534020) from the National Natural Scientific Foundation of China (NNSFC) and the "Bai Ren" Project of the Chinese Academy of Sciences. We acknowledge the support of the National Institute of Standards and Technology, U.S. Department of Commerce, in providing the small-angle scattering facilities used in this work.

**Supporting Information Available:** Surface tensiometry for solutions of MOBS in the presence and absence of PTHC, apparent diffusion coefficient $D_a$ of wormlike micelles before and after polymerization as a function of $x_{PTHC}$, and a Guinier plot of $\ln(Iq)$ versus $q^2$ for polymerized wormlike micelles. This material is available free of charge via the Internet at http://pubs.acs.org.

LA052384I

(41) Tondre, C.; Zana, R. *J. Colloid Interface Sci.* **1978**, *66*, 544.
(42) Lang, J.; Zana, R. *J. Phys. Chem.* **1975**, *79*, 276.
(43) Cochin, D.; Zana, R.; Candau, F. *Macromolecules* **1993**, *26*, 5765.
(44) Aniansson, G. E. A. *Prog. Colloid Polym. Sci.* **1985**, *70*, 2.
(45) Aniansson, E. A. G.; Wall, S. N.; Almgren, M.; Hoffmann, H.; Kielmann, I.; Ulbricht, W.; Zana, R.; Lang, J.; Tondre, C. *J. Phys. Chem.* **1976**, *80*, 905.
(46) Hutchinson, R. A.; Beuermann, S.; Paquet, D. A.; McMinn, J. H. *Macromolecules* **1997**, *30*, 3490.
(47) Maxwell, I. A.; Morrison, B. R.; Napper, D. H.; Gilbert, R. G. *Macromolecules* **1991**, *24*, 1629.
(48) Morgan, J. D.; Kaler, E. W. *Macromolecules* **1998**, *31*, 3197.